Published in final edited form as:
Life Sci. 2009 March 13; 84(11-12): 380–387. doi:10.1016/j.lfs.2009.01.001.

Differential modulation of late sodium current by protein kinase A in R1623Q mutant of LQT3

Takuo Tsurugi[a], **Toshihisa Nagatomo**[a,*], **Haruhiko Abe**[a], **Yasushi Oginosawa**[a], **Hiroko Takemasa**[a], **Ritsuko Kohno**[a], **Naomasa Makita**[b], **Jonathan C. Makielski**[c], and **Yutaka Otsuji**[a]

[a] Second Department of Internal Medicine, University of Occupational and Environmental Health Japan, Kitakyushu 807-8555, Japan

[b] Department of Cardiovascular Medicine, Hokkaido University Graduate School of Medicine, Sapporo 060-8638, Japan

[c] Department of Medicine, Section of Cardiovascular Medicine, University of Wisconsin, Madison, WI 53792, USA

Abstract

Aims—In the type 3 long QT syndrome (LQT3), shortening of the QT interval by overdrive pacing is used to prevent life-threatening arrhythmias. However, it is unclear whether accelerated heart rate induced by β-adrenergic agents produces similar effects on the late sodium current (I_{Na}) to those by overdrive pacing therapy. We analyzed the β-adrenergic-like effects of protein kinase A and fluoride on I_{Na} in R1623Q mutant channels.

Main methods—cDNA encoding either wild-type (WT) or R1623Q mutant of $hNa_v1.5$ was stably transfected into HEK293 cells. I_{Na} was recorded using a whole-cell patch-clamp technique at 23 °C.

Key findings—In R1623Q channels, 2 mM pCPT-AMP and 120 mM fluoride significantly delayed macroscopic current decay and increased relative amplitude of the late I_{Na} in a time-dependent manner. Modulations of peak I_{Na} gating kinetics (activation, inactivation, recovery from inactivation) by fluoride were similar in WT and R1623Q channels. The effects of fluoride were almost completely abolished by concomitant dialysis with a protein kinase inhibitor. We also compared the effect of pacing with that of β-adrenergic stimulation by analyzing the frequency-dependence of the late I_{Na}. Fluoride augmented frequency-dependent reduction of the late I_{Na}, which was due to preferential delay of recovery of late I_{Na}. However, the increase in late I_{Na} by fluoride at steady-state was more potent than the frequency-dependent reduction of late I_{Na}.

Significance—Different basic mechanisms participate in the QT interval shortening by pacing and β-adrenergic stimulation in the LQT3.

Keywords

Arrhythmia; Long QT syndrome; Sodium channel; Protein kinase A

*Corresponding author. Second Department of Internal Medicine, University of Occupational and Environmental Health Japan, 1-1 Iseigaoka, Yahatanishi-ku, Kita-kyushu 807-8555, Japan. Tel.: +81 93 691 7436; fax: +81 93 691 6913. toshi@med.uoeh-u.ac.jp (T. Nagatomo).

Introduction

Congenital long QT syndrome (LQTS) is a hereditary cardiac disorder characterized by prolonged ventricular repolarization, which causes syncope and sudden cardiac death due to life-threatening ventricular tachyarrhythmias. Type 3 of the long QT syndrome (LQT3) is caused by mutations in *SCN5A*, the gene that encodes the α-subunit of the human voltage-dependent cardiac Na^+ channel ($hNa_v1.5$) (Jiang et al., 1994; George et al., 1995; Wang et al., 1995). Previous functional studies of *SCN5A* mutants indicated that most LQT3 mutations cause increased late sodium current (I_{Na}) that results in action potential prolongation and QT lengthening on the surface ECG.

Genotype–phenotype relationships are important for the diagnosis and therapeutic strategy in the LQTS. Ventricular tachyarrhythmias and sudden cardiac death in patients with LQT3 tend to occur during sleep or at rest when the heart rate is slow (Schwartz et al., 1995, 2001). Enhanced shortening of the QT interval by rapid pacing was observed in an experimental model of LQT3 (Priori et al., 1996; Shimizu and Antzelevitch, 1997; Fabritz et al., 2003). The biophysical properties related to this important clinical finding have been reported in particular LQT3 mutations (Clancy and Rudy, 1999; Veldkamp et al., 2000, 2003; Rivolta et al., 2001; Clancy et al., 2002; Nagatomo et al., 2002; Oginosawa et al., 2005). However, it is not clear at this stage whether the increase of heart rate by β-adrenergic agents has effects on the late I_{Na} similar to those of overdrive pacing.

Cardiac voltage-dependent Na^+ channels are modulated by activation of β-adrenergic receptors acting through both direct and indirect pathways (Schubert et al., 1989; Matsuda et al., 1992). The cAMP-dependent protein kinase (protein kinase A, PKA), which is activated by β-adrenergic agents, is one of the major signaling pathways that regulate cardiac Na^+ channel function. In the LQT3 mutant channels, PKA stimulation has little or no effect on the late I_{Na} in Y1795C and Y1795H channels but enhances the late I_{Na} in ΔKPQ and D1790G channels (Chandra et al., 1999; Tateyama et al., 2003b). Thus, the effects of cAMP on the late I_{Na} in LQT3 mutant channels are variable.

A missense mutation of *SCN5A* (R1623Q), in which a charged arginine residue is substituted for a neutral glutamine at an external position of S4 segment of domain IV (DIV-S4), has been identified in a Japanese girl (Miura et al., 2003). The patient has been also reported to develop recurrent ventricular tachycardia and cardiac arrest during sleep and at rest, and cardiac pacing combined with sodium channel blocker effectively prevented the cardiac events (Miura et al., 2003).

In the present study, we investigated the effects of cAMP and a nonspecific phosphatase inhibitor fluoride, which mimics the effects of β-adrenergic agents (Chandra et al., 1999; Tateyama et al., 2003b), on the late I_{Na} in the R1623Q mutant channels. The late I_{Na} was preferentially enhanced compared with peak I_{Na} by continuous application of pCPT-AMP or fluoride. Although frequency-dependent reduction for the late I_{Na} was augmented by fluoride, the overall amplitude of the late I_{Na} was increased by fluoride.

Materials and methods

Clones and construction of R1623Q mutation

Amino acid substitution of glutamine for arginine-1623 (R1623Q) of human cardiac Na^+ channel α-subunit ($hNa_v1.5$) was performed by an overlap extension polymerase chain reaction (PCR). The 459-bp cDNA of $hNa_v1.5$ was amplified using oligonucleotide primers $hNa_v1.5$-4418F (5′-TCAACCAACAGAAGAAAAAGT-3′) and R1623Q-R (5′-GGATGACTT-GGAA-GAGCGTCGG-3′). Similarly, the 165-bp cDNA of $hNa_v1.5$ was

amplified using oligonucleotide primers R1623Q-F (5′-CTCTTCCAAGT-CATCCGCCTG-3′) and hNa$_v$1.5-5006R (5′-GCCAAAGATGGAGTAGATGA-3′). Subsequently, the two PCR products were purified and combined in a second round of PCR with the primer pair hH-4418-F and hNa$_v$1.5-5006R. A 608-bp PCR product was digested with BamHI/BstEII and subcloned back into WT-hNa$_v$1.5 to assemble the R1623Q-hNa$_v$1.5 construct as reported previously (Makita et al.,1998). The entire PCR generated region was sequenced completely. We confirmed the mutation and the lack of any unwanted changes in the channel.

Cell preparation and transfection

Approximately 5×10^5 cells from a transformed HEK293 were seeded on a 60-mm diameter plate with 3 ml of culture medium one day before the transfection. The culture medium was MEM complete medium containing minimum essential medium (Eagle's salts and L-glutamine), 10% of fetal bovine serum, 2 mM L-glutamine, 0.1 mM MEM non-essential amino acids solution, 1 mM MEM pyruvate solution, 10,000 U penicillin and 10,000 μg streptomycin. Transfection for WT-hNa$_v$1.5 was carried out by the cationic liposome method, as described previously (Nagatomo et al., 1998). The cDNA for R1623Q-hNa$_v$1.5 was transfected into HEK293 cells using LipofectAMINE™2000 (Invitrogen, San Diego, CA) as directed by the manufacturer. To select stably transfected cells, geneticine (G418 sulfate) at a concentration of 800 μg/ml was added for approximately 15 days, at which time surviving single colonies were isolated and cultured with 400 μg/ml geneticine for 1–3 weeks.

Electrophysiological recordings

Macroscopic sodium current (I_{Na}) was recorded using the whole-cell patch-clamp technique at room temperature (23±1 °C). The bath solution contained (in mM): NaCl 140, KCl 4, $CaCl_2$ 1.8, $MgCl_2$ 0.75 and HEPES 5 (pH 7.4 set with NaOH). The pipette solution contained (in mM): CsF 120, CsCl 20, EGTA 5 and HEPES 5 (pH 7.4 set with CsOH). Pipettes had resistances between 1.0 and 1.2 MΩ when filled with the above electrode solution. Membrane currents were recorded with an Axopatch 200A amplifier (Axon Instruments Inc., Union City, CA). Data were acquired using Clampex ver. 9.2 (Axon Instruments Inc.), then digitized at 100 kHz and low-pass filtered at 10 kHz. The methods used to achieve and verify voltage control methods were those published previously (Nagatomo et al., 1998). Selective activator of cAMP dependent protein kinase, 8-(4-chlorophenylthio) adenosine 3′:5′-cyclic mono phosphate (pCPT-cAMP), and the cAMP-dependent protein kinase inhibitor (PKI) were purchased from Sigma-Aldrich (St. Louis, MO) and dissolved in bath solution (2 mM) and pipette solution (20 μM), respectively. The effects of pCPT-cAMP were examined in the presence of intrapipette fluoride (120 mM) because the current recordings were not stable in the absence of intrapipette fluoride.

Data analysis

Passive leak subtraction of peak and late I_{Na} was performed as previously described (Nagatomo et al., 1998). Data were fit to model equations using non-linear regression with pClamp ver. 9.2 (Axon Instruments Inc.) or Sigma Plot ver. 9.0 (SPSS Science, Chicago, IL). Goodness of fit was judged both visually and by the sum of squares errors. The time course of macroscopic current decay after 90% of peak was fit with double-exponential function: $I_{Na}(t)=1-[A_f\times\exp(-t/\tau_f)+A_s\times\exp(-t/\tau_s)]+\text{offset}$, where t is time, τ_f and τ_s represent the time constants of the fast and slow components, and A_f and A_s are fractions of each component, respectively. Steady-state inactivation and activation data were fit with the Boltzmann function: Normalized $I_{Na} = [1 + \exp(V - V_{1/2})/\kappa]^{-1}$; Normalized $G_{Na} = [1 + \exp(V_{1/2} - V)/\kappa]^{-1}$, where $V_{1/2}$ and κ are half-maximum voltage and the slope factor, respectively. For activation curve, conductance (G_{Na}) was calculated from peak I_{Na} divided by the driving force and normalized to the peak

conductance. Recovery from inactivation was analyzed by fitting data with double-exponential function: Normalized $I_{Na} = A_f \times \exp(-t/\tau_f) + A_s \times \exp(-t/\tau_s) + (\text{offset})$, where t is a recovery time interval, τ_f and τ_s are the fast and slow time constants, A_f and A_s are the fractions of recovery components, and offset is a non-inactivating component. Data are expressed as mean±standard error (SEM) with n representing the number of cells. Differences between two groups were examined for statistical significance using the Student's t-test, while those among multiple groups were examined by one-way ANOVA. A P value of <0.05 was considered statistically significant.

Results

Effects of cAMP on WT and R1623Q channels

Fig. 1A shows representative current recordings from HEK293 cells expressing wild-type (WT) and R1623Q mutant channels at baseline and 10 min after perfusion of cells with pCPT-cAMP (2 mM) in the presence of intrapipette fluoride. Currents were elicited by 250 ms step pulse to −20 mV from a holding potential of −150 mV. In R1623Q channels, the macroscopic current decay was delayed and the late I_{Na} was significantly increased in the presence of pCPT-cAMP. However, the effects of pCPT-cAMP on late I_{Na} in WT were negligible. The peak I_{Na} was not affected by pCPT-cAMP in both WT and R1623Q channels. Table 1 lists the time constants for fast (τ_f) and slow (τ_s) components of the current decay. The late I_{Na} in R1623Q channels measured as the mean value of the current amplitude between 39 and 41 ms was increased in a time-dependent manner and more than doubled to the baseline amplitude at 15 min after the application of pCPT-cAMP (Fig. 1B). Fig. 1C shows changes in fraction of late I_{Na} (normalized to peak I_{Na}) at baseline and at 10 min after application of pCPT-cAMP. The fraction of the late I_{Na} in R1623Q channels was significantly higher than that at baseline (P<0.05). These results suggest that cAMP-dependent phosphorylation preferentially increases the late I_{Na} in R1623Q channels.

Effects of fluoride on WT and R1623Q channels

Since intracellular fluoride acts as a nonspecific phosphatase inhibitor, we tested whether it could mimic the effect of pCPT-cAMP by buffering phosphorylation-dependent changes in channel activity. Fig. 2A demonstrates that intrapipette fluoride delayed macroscopic current decay and increased the late I_{Na} in R1623Q channels but not in WT channels. The fluoride-induced increase in late I_{Na} was almost completely prevented by concomitant dialysis with cAMP-dependent protein kinase inhibitor (PKI) at 20 μM. Table 1 summarizes the time constants for fast (τ_f) and slow (τ_s) components of the current decay. In R1623Q channels, the late I_{Na} increased in a time-dependent manner and approximately doubled after dialysis with fluoride although the augmentation was weaker than that with pCPT-cAMP plus fluoride (Figs. 1B and 2B). The peak I_{Na} was not affected by fluoride in both WT and R1623Q channels. Fig. 2C shows summary data of changes in the fraction of late I_{Na}. Fluoride significantly increased the fraction of the late I_{Na} in R1623Q channels ($P < 0.05$). These results suggest that the increase in late I_{Na} was due to PKA-dependent phosphorylation in R1623Q channels and that fluoride acts as an endogenous phosphatase inhibitor in HEK cells.

Kinetic modulation by fluoride

We used intrapipette fluoride to investigate kinetic modulation by PKA-dependent phosphorylation. Currents recordings were started at 5 min after achieving the whole-cell configuration. Fig. 3 shows representative current tracings and current–voltage relationships for WT and R1623Q channels. Fluoride again delayed macroscopic current decay in the R1623Q channels but not in WT channels. However, fluoride shifted the peak of the current–voltage relationship in a negative direction in both WT and R1623Q channels. These effects by fluoride were not seen in experiments using concomitant dialysis with PKI.

Fig. 4A shows the results of steady-state inactivation and activation for WT and R1623Q channels. The voltage dependence of steady-state inactivation was assessed by a two-pulse protocol as indicated in the protocol diagram in Fig. 4A. Peak I_{Na} was measured at a test potential of −20 mV after 1 s-long conditioning potentials between −150 and −40 mV, and normalized to the largest peak I_{Na} obtained. The voltage dependence of activation was evaluated as a normalized peak conductance–voltage relationship (see Methods). Fluoride significantly shifted the half-maximum voltages ($V_{1/2}$) of the steady-state inactivation and the activation curves in negative directions in both WT and R1623Q channels and these shifts by fluoride were significantly attenuated by concomitant dialysis with PKI. The slope factor (κ) was not significantly different in the presence of fluoride. Table 2 summarizes the above parameters at steady-state inactivation and activation of the WT and R1623Q channels.

We also studied the recovery from inactivation using the two-pulse protocol (Fig. 4B). The membrane potential was stepped to −20 mV from a holding potential of −120 mV for 500 ms, and a test pulse to −20 mV was delivered followed by a variable recovery interval. The time constants and their fraction are summarized in Table 3. Fluoride significantly increased the fast time constants in both WT and the R1623Q channels. Since the time constants were not significantly different between the peak and late I_{Na} in the R1623Q channels (Oginosawa et al., 2005), we also tested the effect of fluoride on recovery from inactivation for the late I_{Na}. Interestingly, the time constants of recovery and the fraction of slow component of the late I_{Na} were preferentially increased by fluoride compared with those of the peak I_{Na} ($P < 0.05$).

Frequency-dependent reduction of peak and late I_{Na}

Cumulative inactivation and slow recovery of late I_{Na} for ΔKPQ mutant channels might underlie rate-dependent decreases in late I_{Na} and shortening of the QT interval at higher rates (Nagatomo et al., 1998); we therefore investigated the effects of fluoride on the frequency-dependence of peak and late I_{Na} in R1623Q channels. Fig. 5A shows representative current recordings in response to a train of 50 pulses with fluoride in the presence or absence of PKI at 2 Hz. Fluoride augmented the frequency-dependent reduction of peak and late I_{Na} compared with those with PKI (Fig. 5B). Although fluoride augmented the frequency-dependent reduction of peak and late I_{Na} compared with those in the presence of PKI, the frequency-dependent reduction of late I_{Na} was more preferentially enhanced compared with peak I_{Na} at both 1 Hz and 2 Hz.

Analysis of fluoride effects

We have demonstrated opposing effects for fluoride on the late I_{Na} in R1623Q channels; i.e., steady-state increase of late I_{Na} versus augmented frequency-dependent reduction of late I_{Na}. To investigate which effect predominates in modulating the late I_{Na}, we compared the relative amplitude of the late I_{Na} for the 50th pulse under steady-state fluoride stimulation with and without PKI (20 μM). Fig. 6A shows the serial changes in relative amplitude of the late I_{Na} (late/peak I_{Na}) in response to a train of 50 pulses recorded at 5 min after achieving stable whole-cell configuration. Fluoride enhanced the frequency-dependent reduction of late/peak I_{Na}, but its effect of steady-state increase of the late/peak I_{Na} was more potent.

Discussion

In the present study, we investigated the effects of cAMP and fluoride on late I_{Na} and the I_{Na} kinetics in R1623Q mutant channels. In the R1623Q channels, cAMP and fluoride increased sustained late I_{Na} in a time-dependent manner. On the other hand, fluoride augmented the frequency-dependent reduction of the late I_{Na}. Comparison of the opposite effects of cAMP and fluoride indicates that the increase of the late I_{Na} was more potent than the augmentation of frequency- dependent reduction of late I_{Na} in our experimental condition.

cAMP modulates late I_{Na} in R1623Q mutant channels

In the LQT3 Na^+ channels, PKA stimulation has been reported to have little or no effect on the late I_{Na} in Y1795C and Y1795H channels but to enhance the late I_{Na} in ΔKPQ and D1790G channels (Chandra et al., 1999; Tateyama et al., 2003b). Tateyama et al. (2003b) proposed that interactions among multiple cytoplasmic components of the channel contributed to the functional consequences of PKA-dependent modulation of the late I_{Na}. Since the mutated site of the R1623Q in the present study is located at an external position of the S4 segment of domain IV, this site might also contribute to the PKA-dependent modulation of the late I_{Na}.

cAMP-dependent protein kinase (protein kinase A, PKA) activated by β-adrenergic agents is a major signaling pathway that regulates cardiac Na^+ channel function. However, conflicting results have been reported regarding modulation of cardiac Na^+ current by β-adrenergic stimulation. Treatment of mammalian myocytes with cAMP-elevating agents or membrane permeable cAMP analogs has been shown to cause either a decrease (Schubert et al., 1989, 1990; Ono et al., 1989; Sunami et al., 1991) or increase (Matsuda et al., 1992; Tytgat et al., 1990; Lu et al., 1999) in Na^+ current. The different effects of PKA on cardiac Na^+ channel activity might depend on experimental conditions (*e.g.*, species, developmental changes and pulse protocols). The holding and test potentials in the pulse protocol are particularly important when investigating the effects of cAMP on I_{Na} (Kirstein et al., 1991; Ono et al., 1993; Muramatsu et al., 1994). In the present study, we observed a negative shift in inactivation and conductance curves after application of fluoride, which mimicked the effect of cAMP, in both WT and R1623Q channels (Fig. 4). The results are in good agreement with the data reported by several laboratories and suggest that peak I_{Na} should be decreased by cAMP at physiological resting membrane potential usually from −80 to −100 mV because of a decrease in channel availability. In fact, peak I_{Na} in ΔKPQ mutant channels was reduced with holding potential of −90 mV but the relative late I_{Na} to peak I_{Na} was increased (Chandra et al., 1999), and we also observed a decrease in peak I_{Na} with a holding potential of −90 mV while the relative late I_{Na} was increased (data not shown). Therefore, we used a holding potential of −150 mV and a test potential of −20 mV to discriminate the effects of cAMP on peak I_{Na} with that on late I_{Na}. Using this protocol, cAMP preferentially increased the late I_{Na} without significantly changing the peak I_{Na}.

Two residues (S525, S528) in the domain I–II linker of cardiac Na^+ channel α-subunit are considered important consensus sites for cAMP-dependent phosphorylation (Murphy et al., 1996). The R1623Q mutation results in replacement of neutral glutamine for positively charged arginine-1623Q located at the outermost of the S4 segment of domain IV (DIV-S4). This region is not only part of the voltage sensor of channel activation, but also important for activation–inactivation coupling (Cha et al., 1999; Sheets et al., 2000). The loss of the positive charge of this site changes the voltage dependence of channel gating resulting in less voltage sensitivity of steady-state inactivation and alternative recovery from inactivation in the R1623Q mutant channels (Makita et al., 1998; Kambouris et al., 1998, 2000; Oginosawa et al., 2005). In the present study, fluoride modulated activation, inactivation and recovery from inactivation of the peak I_{Na} in a similar degree in both WT and R1623Q channels. Unremarkable mutation-induced changes in peak I_{Na} gating by cAMP have been also reported for ΔKPQ and D1790G channels (Chandra et al., 1999; Tateyama et al., 2003b). It is possible that the mutated sites in R1623Q do not directly interact with the PKA consensus sites in domain I–II linker of the cardiac Na^+ channel α-subunit. On the other hand, the late I_{Na} in R1623Q channels was selectively increased by cAMP and fluoride compared with the peak I_{Na} for R1623Q, suggesting independence of the effects of cAMP on the late I_{Na}. In the D1790G mutant channel, loss of negative charge or replacement to positive charge at residue 1790 has been reported to be an important determinant of the enhancement of late I_{Na} (Tateyama et al., 2003b). Thus, loss of negative charge on the cytoplasmic surface or loss of positive charge on the domain IV

would worsen the activation–inactivation coupling, resulting in enhancement of the late I_{Na} under PKA-dependent phosphorylation.

Interestingly, our results showed that the frequency-dependent reduction of the late I_{Na} was preferentially augmented by fluoride compared with peak I_{Na} under PKA activation. This effect on the late I_{Na} in R1623Q channels was not observed in control conditions (Oginosawa et al., 2005). The underlying mechanism was mainly the preferential delay of recovery compared with peak I_{Na} under PKA activation, suggesting again the independence of the effects of cAMP on the late I_{Na} kinetics in R1623Q channels.

Clinical implications and limitations of the study

Clinical studies indicate that ventricular tachyarrhythmias and sudden cardiac death in LQT3 patients tend to occur during sleep or at rest when the heart rate is slow, and that prevention of bradycardia is one of the main therapeutic strategies in patients with LQT3 (Schwartz et al., 1995, 2001). Furthermore, cardiac overdrive pacing is effective in shortening the QT interval in LQT patients and in experimental models of the LQT3 (Priori et al., 1996; Shimizu and Antzelevitch, 1997). In the transgenic mice of the ΔKPQ mutant of LQT3, cardiac pacing is also effective to decrease the dispersion of action potential duration and suppress early after depolarization (Fabritz et al., 2003). On the other hand, sympathetic stimulation with isoproterenol or epinephrine shortened the action potential duration in experimental models of LQT3 (Priori et al., 1996; Shimizu and Antzelevitch, 2000). In addition, provocation testing with epinephrine is used to diagnose and unmask LQTS (Noda et al., 2002; Vyas et al., 2006). Based on these observations, we initially hypothesized that the late I_{Na} would decrease in response to β-adrenergic stimulation. Contrary to our expectations, the late I_{Na} increased in response to cAMP in the present study. Our results in R1623Q mutant channel are in agreement with those of previous studies (Chandra et al., 1999; Tateyama et al., 2003b), which also reported that cAMP increased the late I_{Na} in ΔKPQ and D1790G mutant channels. β-adrenergic stimulation with isoproterenol is known to augment various currents, including slow component of the delayed rectifier K^+ current (I_{Ks}), Ca^{2+}-activated chloride current, L-type Ca^{2+} current, and Na^+/Ca^{2+} exchange current. Since the response of action potential duration and of the QT to β-adrenergic stimulation largely depends on the balance of these currents, augmentation of inward current including the late I_{Na} might be weaker than that of outward currents under β-adrenergic stimulation.

The present study has certain limitations and caution must be taken in extrapolating the present results to the clinical settings. We used $hNa_v1.5$ channels heterologously expressed in a human cell line. The possible effects of cAMP on other ion channels should be considered. In addition, effects of catecholamines do not limit to the β-adrenergic stimulation. Stimulation of protein kinase C via α-adrenergic receptor reduces the late I_{Na} in Y1795C, Y1795H and ΔKPQ mutants of LQT3 (Tateyama et al., 2003a). Further data in cardiomyocytes or in vivo data are needed to identify the effects of cAMP and catecholamines. Secondly, we used the frequencies at 1 and 2 Hz that selected based on the clinical setting of the pacemaker (50 to 120 pace/min). However, frequency at 3 Hz, for example, might emphasize the frequency-dependent reduction by fluoride (pacing effect) and overridden steady-state increase of late I_{Na} by fluoride (baseline effect). Finally, we performed experiments at room temperature. Temperature might influence the gating characteristics of I_{Na} and consequently the balance between the steady-state increase in late I_{Na} and its frequency-dependent reduction.

Conclusion

Different mechanisms are involved in QT interval shortening induced by pacing and β-adrenergic stimulation. The mechanism of QT shortening by overdrive pacing might mainly include a frequency-dependent reduction of the late and phase 3 I_{Na} in R1623Q mutant

channels, while a balance of inward and outward currents might explain the QT interval shortening by β-adrenergic stimulation.

Acknowledgments

This work was supported by a Grant-in Aid for Scientific Research from the Ministry of Education, Culture, Sports, Science and Technology, Japan (to T.N. 17590194).

References

Cha A, Ruben PC, George AL Jr, Fujimoto E, Bezanilla F. Voltage sensors in domains III and IV, but not I and II, are immobilized by Na^+ channel fast inactivation. Neuron 1999;22 (1):73–87. [PubMed: 10027291]

Chandra R, Chauhan VS, Starmer CF, Grant AO. β-adrenergic action on wild-type and KPQ mutant human cardiac Na^+ channels: shift in gating but no change in Ca^{2+}:Na^+ selectivity. Cardiovascular Research 1999;42 (2):490–502. [PubMed: 10533584]

Clancy CE, Rudy Y. Linking a genetic defect to its cellular phenotype in a cardiac arrhythmia. Nature 1999;400 (6744):566–569. [PubMed: 10448858]

Clancy CE, Tateyama M, Kass RS. Insights into the molecular mechanisms of bradycardia-triggered arrhythmias in long QT-3 syndrome. The Journal of Clinical Investigation 2002;110 (9):1251–1262. [PubMed: 12417563]

Fabritz L, Kirchhof P, Franz MR, Nuyens D, Rossenbacker T, Ottenhof A, Haverkamp W, Breithardt G, Carmeliet E, Carmeliet P. Effect of pacing and mexiletine on dispersion of repolarisation and arrhythmias in ΔKPQ SCN5A (long QT3) mice. Cardiovascular Research 2003;57 (4):1085–1093. [PubMed: 12650887]

George AL Jr, Varkony TA, Drabkin HA, Han J, Knops JF, Finley WH, Brown GB, Ward DC, Haas M. Assignment of the human heart tetrodotoxin-resistant voltage-gated Na^+ channel alpha-subunit gene (SCN5A) to band 3p21. Cytogenetics and cell genetics 1995;68 (1–2):67–70. [PubMed: 7956363]

Jiang C, Atkinson D, Towbin JA, Splawski I, Lehmann MH, Li H, Timothy K, Taggart RT, Schwartz PJ, Vincent GM, Moss AJ, Keating MT. Two long QT syndrome loci map to chromosomes 3 and 7 with evidence for further heterogeneity. Nature genetics 1994;8 (2):141–147. [PubMed: 7842012]

Kambouris NG, Nuss HB, Johns DC, Tomaselli GF, Marban E, Balser JR. Phenotypic characterization of a novel long-QT syndrome mutation (R1623Q) in the cardiac sodium channel. Circulation 1998;97 (7):640–644. [PubMed: 9495298]

Kambouris NG, Nuss HB, Johns DC, Marban E, Tomaselli GF, Balser JR. A revised view of cardiac sodium channel “blockade” in the long-QT syndrome. The Journal of Clinical Investigation 2000;105 (8):1133–1140. [PubMed: 10772658]

Kirstein M, Eickhorn R, Langenfeld H, Kochsiek K, Antoni H. Influence of β-adrenergic stimulation on the fast sodium current in the intact rat papillary muscle. Basic Research in Cardiology 1991;86 (5): 441–448. [PubMed: 1662947]

Lu T, Lee HC, Kabat JA, Shibata EF. Modulation of rat cardiac sodium channel by the stimulatory G protein alpha subunit. The Journal of Physiology 1999;518 (Pt 2):371–384. [PubMed: 10381586]

Makita N, Shirai N, Nagashima M, Matsuoka R, Yamada Y, Tohse N, Kitabatake A. A de novo missense mutation of human cardiac Na^+ channel exhibiting novel molecular mechanisms of long QT syndrome. FEBS Letters 1998;423 (1):5–9. [PubMed: 9506831]

Matsuda JJ, Lee H, Shibata EF. Enhancement of rabbit cardiac sodium channels by β-adrenergic stimulation. Circulation Research 1992;70 (1):199–207. [PubMed: 1309315]

Miura M, Yamagishi H, Morikawa Y, Matsuoka R. Congenital long QT syndrome and 2:1 atrioventricular block with a mutation of the SCN5A gene. Pediatric Cardiology 2003;24 (1):70–72. [PubMed: 12574983]

Muramatsu H, Kiyosue T, Arita M, Ishikawa T, Hidaka H. Modification of cardiac sodium current by intracellular application of cAMP. Pflügers Archiv: European Journal of Physiology 1994;426 (1–2):146–154.

Murphy BJ, Rogers J, Perdichizzi AP, Colvin AA, Catterall WA. cAMP-dependent phosphorylation of two sites in the alpha subunit of the cardiac sodium channel. The Journal of Biological Chemistry 1996;271 (46):28837–28843. [PubMed: 8910529]

Nagatomo T, Fan Z, Ye B, Tonkovich GS, January CT, Kyle JW, Makielski JC. Temperature dependence of early and late currents in human cardiac wild-type and long Q-T ΔKPQ Na^+ channels. American Journal of Physiology 1998;275 (6 Pt 2):H2016–2024. [PubMed: 9843800]

Nagatomo T, January CT, Ye B, Abe H, Nakashima Y, Makielski JC. Rate-dependent QT shortening mechanism for the LQT3 ΔKPQ mutant. Cardiovascular Research 2002;54 (3):624–629. [PubMed: 12031708]

Noda T, Takaki H, Kurita T, Suyama K, Nagaya N, Taguchi A, Aihara N, Kamakura S, Sunagawa K, Nakamura K, Ohe T, Horie M, Napolitano C, Towbin JA, Priori SG, Shimizu W. Gene-specific response of dynamic ventricular repolarization to sympathetic stimulation in LQT1, LQT2 and LQT3 forms of congenital long QT syndrome. European Heart Journal 2002;23 (12):975–983. [PubMed: 12069453]

Oginosawa Y, Nagatomo T, Abe H, Makita N, Makielski JC, Nakashima Y. Intrinsic mechanism of the enhanced rate-dependent QT shortening in the R1623Q mutant of the LQT3 syndrome. Cardiovascular Research 2005;65 (1):138–147. [PubMed: 15621041]

Ono K, Kiyosue T, Arita M. Isoproterenol, DBcAMP, and forskolin inhibit cardiac sodium current. American Journal of Physiology 1989;256 (6 Pt 1):C1131–1137. [PubMed: 2544093]

Ono K, Fozzard HA, Hanck DA. Mechanism of cAMP-dependent modulation of cardiac sodium channel current kinetics. Circulation Research 1993;72 (4):807–815. [PubMed: 8383015]

Priori SG, Napolitano C, Cantu F, Brown AM, Schwartz PJ. Differential response to Na^+ channel blockade, β-adrenergic stimulation, and rapid pacing in a cellular model mimicking the SCN5A and HERG defects present in the long-QT syndrome. Circulation Research 1996;78 (6):1009–1015. [PubMed: 8635231]

Rivolta I, Abriel H, Tateyama M, Liu H, Memmi M, Vardas P, Napolitano C, Priori SG, Kass RS. Inherited Brugada and long QT-3 syndrome mutations of a single residue of the cardiac sodium channel confer distinct channel and clinical phenotypes. The Journal of Biological Chemistry 2001;276 (33):30623–30630. [PubMed: 11410597]

Schubert B, VanDongen AM, Kirsch GE, Brown AM. β-adrenergic inhibition of cardiac sodium channels by dual G-protein pathways. Science 1989;245 (4917):516–519. [PubMed: 2547248]

Schubert B, Vandongen AM, Kirsch GE, Brown AM. Inhibition of cardiac Na^+ currents by isoproterenol. American Journal of Physiology 1990;258 (4 Pt 2):H977–982. [PubMed: 2158748]

Schwartz PJ, Priori SG, Locati EH, Napolitano C, Cantu F, Towbin JA, Keating MT, Hammoude H, Brown AM, Chen LS. Long QT syndrome patients with mutations of the SCN5A and HERG genes have differential responses to Na^+ channel blockade and to increases in heart rate. Implications for gene-specific therapy. Circulation 1995;92 (12):3381–3386. [PubMed: 8521555]

Schwartz PJ, Priori SG, Spazzolini C, Moss AJ, Vincent GM, Napolitano C, Denjoy I, Guicheney P, Breithardt G, Keating MT, Towbin JA, Beggs AH, Brink P, Wilde AA, Toivonen L, Zareba W, Robinson JL, Timothy KW, Corfield V, Wattanasirichaigoon D, Corbett C, Haverkamp W, Schulze-Bahr E, Lehmann MH, Schwartz K, Coumel P, Bloise R. Genotype–phenotype correlation in the long-QT syndrome: gene-specific triggers for life-threatening arrhythmias. Circulation 2001;103 (1): 89–95. [PubMed: 11136691]

Sheets MF, Kyle JW, Hanck DA. The role of the putative inactivation lid in sodium channel gating current immobilization. The Journal of General Physiology 2000;115 (5):609–620. [PubMed: 10779318]

Shimizu W, Antzelevitch C. Sodium channel block with mexiletine is effective in reducing dispersion of repolarization and preventing torsade des pointes in LQT2 and LQT3 models of the long-QT syndrome. Circulation 1997;96 (6):2038–2047. [PubMed: 9323097]

Shimizu W, Antzelevitch C. Differential effects of beta-adrenergic agonists and antagonists in LQT1, LQT2 and LQT3 models of the long QT syndrome. Journal of the American College of Cardiology 2000;35 (3):778–786. [PubMed: 10716483]

Sunami A, Fan Z, Nakamura F, Naka M, Tanaka T, Sawanobori T, Hiraoka M. The catalytic subunit of cyclic AMP-dependent protein kinase directly inhibits sodium channel activities in guinea-pig ventricular myocytes. Pflügers Archiv: European Journal of Physiology 1991;419 (3–4):415–417.

Tateyama M, Kurokawa J, Terrenoire C, Rivolta I, Kass RS. Stimulation of protein kinase C inhibits bursting in disease-linked mutant human cardiac sodium channels. Circulation 2003a;107 (25):3216–3222. [PubMed: 12796143]

Tateyama M, Rivolta I, Clancy CE, Kass RS. Modulation of cardiac sodium channel gating by protein kinase A can be altered by disease-linked mutation. Journal of Biological Chemistry 2003b;278 (47): 46718–46726. [PubMed: 14500710]

Tytgat J, Vereecke J, Carmeliet E. A combined study of sodium current and T-type calcium current in isolated cardiac cells. Pflügers Archiv: European Journal of Physiology 1990;417 (2):142–148.

Veldkamp MW, Viswanathan PC, Bezzina C, Baartscheer A, Wilde AA, Balser JR. Two distinct congenital arrhythmias evoked by a multidysfunctional Na(+) channel. Circulation Research 2000;86 (9):E91–97. [PubMed: 10807877]

Veldkamp MW, Wilders R, Baartscheer A, Zegers JG, Bezzina CR, Wilde AA. Contribution of sodium channel mutations to bradycardia and sinus node dysfunction in LQT3 families. Circulation Research 2003;92 (9):976–983. [PubMed: 12676817]

Vyas H, Hejlik J, Ackerman MJ. Epinephrine QT stress testing in the evaluation of congenital long-QT syndrome: diagnostic accuracy of the paradoxical QT response. Circulation 2006;113 (11):1385–1392. [PubMed: 16534005]

Wang Q, Shen J, Splawski I, Atkinson D, Li Z, Robinson JL, Moss AJ, Towbin JA, Keating MT. SCN5A mutations associated with an inherited cardiac arrhythmia, long QT syndrome. Cell 1995;80 (5):805–811. [PubMed: 7889574]

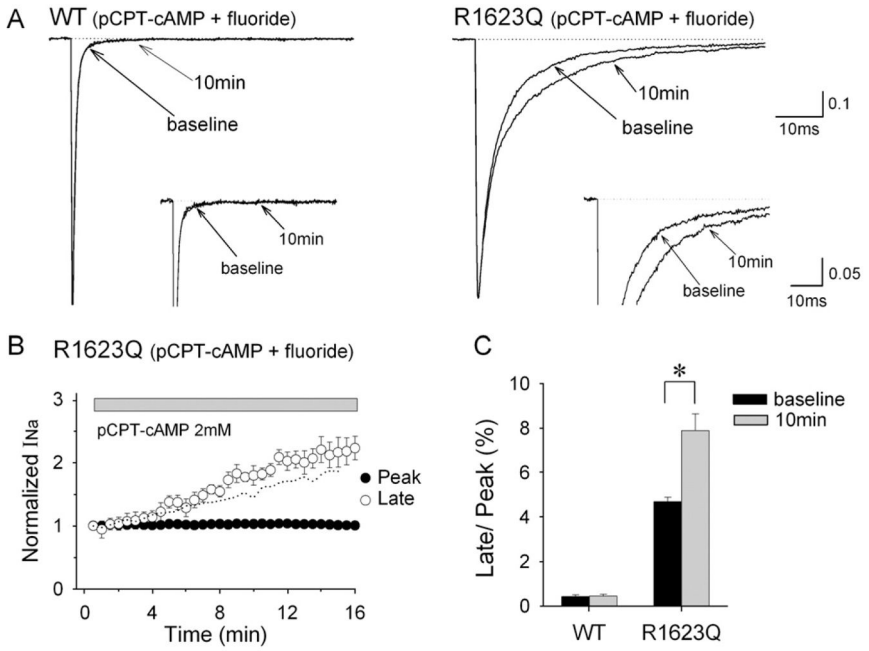

Fig. 1.

Selective increase in late I_{Na} in R1623Q channels by pCPT-cAMP in the presence of intrapipette fluoride. (A) Normalized whole-cell Na^+ current (I_{Na}) in response to 2 mM pCPT-cAMP in cells expressing WT (left) or R1623Q (right) channels. Currents were recorded at baseline (0 min) and 10 min after application of pCPT-cAMP. Inset panels show I_{Na} at different amplitude (peak I_{Na} off scale) and time resolution to emphasize late I_{Na}. (B) Time courses of peak and late I_{Na} for R1623Q channels in response to pCPT-cAMP. Peak (closed circles) and late (open circles) I_{Na} were normalized to the current amplitude at baseline. Application of pCPT-cAMP commenced when the I_{Na} become stable (3 min). Late I_{Na} amplitude was evaluated by using the mean value of the current amplitude between 39 and 41 ms. Dotted line represents the time course of late I_{Na} in the presence of fluoride duplicated from Fig. 2B. (C) The percentage of late I_{Na} relative to peak I_{Na} of WT and R1623Q channels at baseline and 10 min after application of pCPT-cAMP. Data are mean±SEM. WT (n=5), R1623Q (n=5), *P<0.05.

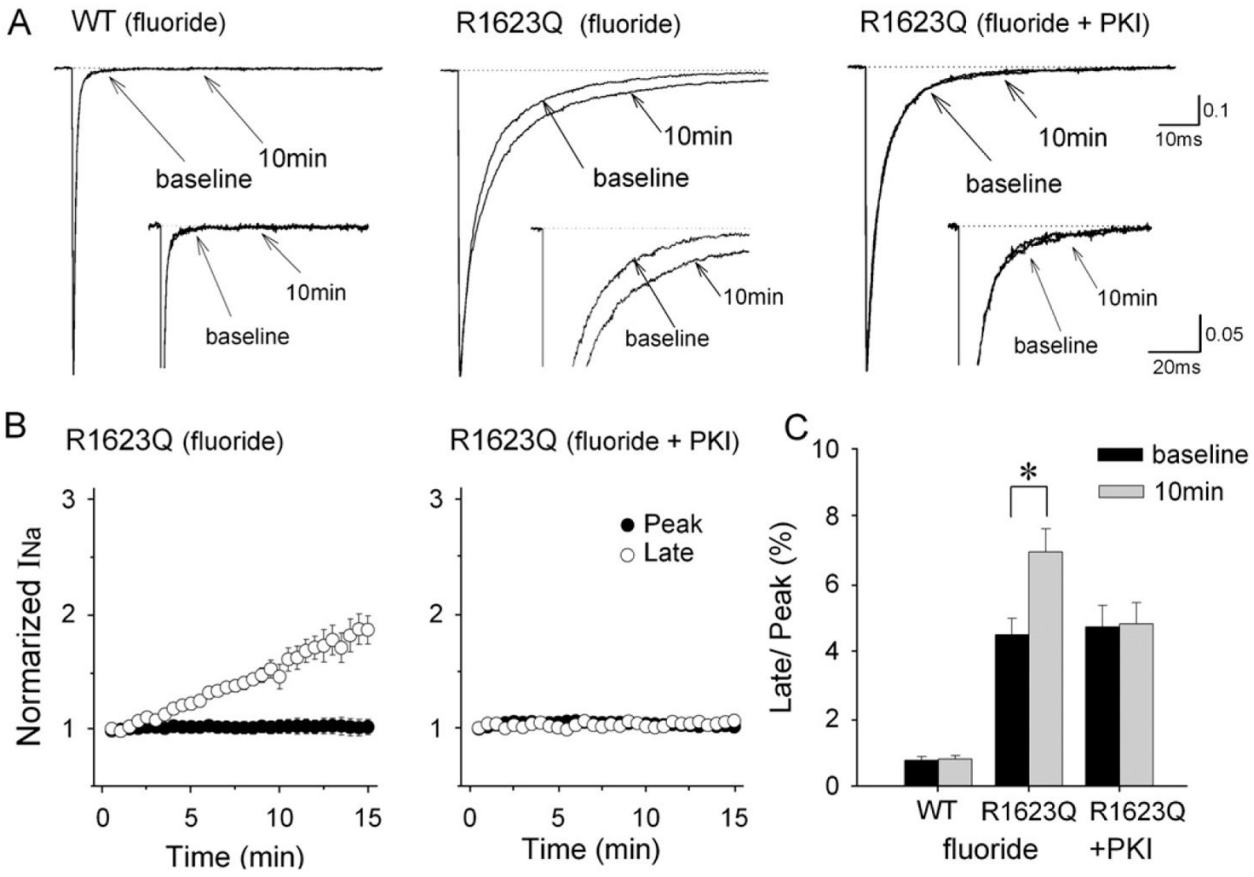

Fig. 2.

Fluoride selectively increases late I_{Na} in R1623Q channels. (A) Normalized whole-cell I_{Na} recorded in cells expressing WT (left) and R1623Q (right) channels in the presence of fluoride (120 mM) in the recording pipette. Currents were recorded at baseline (0 min) and 10 min after establishing whole-cell configurations. Fluoride increased the late I_{Na} in R1623Q channels, which was inhibited by concomitant dialysis of a protein kinase inhibitor (PKI). Inset panels show I_{Na} at different amplitude (peak I_{Na} off scale) and time resolution to emphasize late I_{Na}. (B) Time courses of peak and late I_{Na} for R1623Q channels with intrapipette fluoride. Peak (closed circles) and late (open circles) I_{Na} were normalized to the current amplitude at baseline. PKI at 20 μM abolished fluoride-induced increase in late I_{Na}. (C) Summary data of normalized late I_{Na} at baseline and 10 min after establishing whole- cell configurations with intrapipette fluoride and fluoride plus PKI. Experiments with PKI were conducted only in R1623Q channels. Data are mean±SEM. WT (n=7), R1623Q: fluoride (n=8), R1623Q: fluoride +PKI (n=6), *P<0.05.

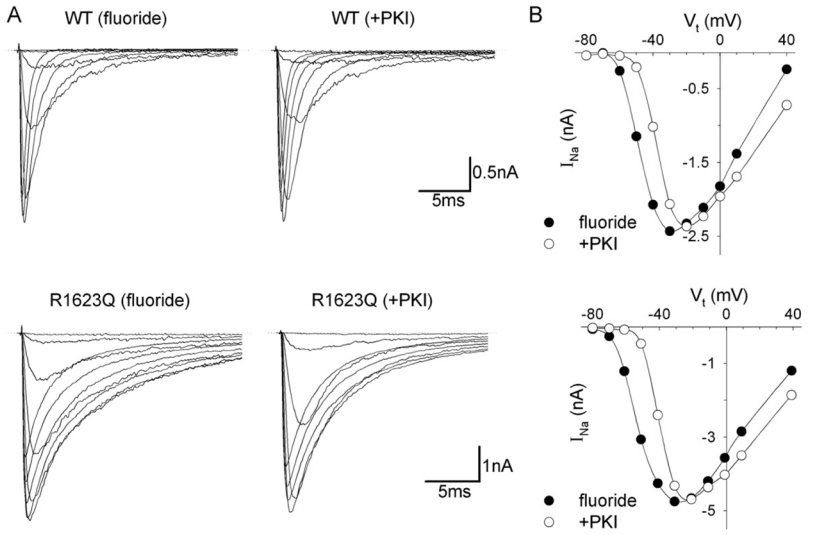

Fig. 3.

Whole-cell I_{Na} for WT and R1623Q channels with intrapipette fluoride in the presence or absence of PKI (20 μM). (A) Current recording obtained at different test potentials (Vt) between −80 and 40 mV from a holding potential of −150 mV from 4 representative cells. Currents with comparable peak amplitudes are shown on the same scale for WT and R1623Q channels. (B) Current–voltage relationship of peak I_{Na} for WT (upper panel) and R1623Q (lower panel) channels for the same cells in (A). The peak of the current–voltage relationship shifted in a negative direction in both WT and R1623Q channels in the presence of fluoride (closed circles), and this effect was inhibited by the application of 20 μM PKI (open circles).

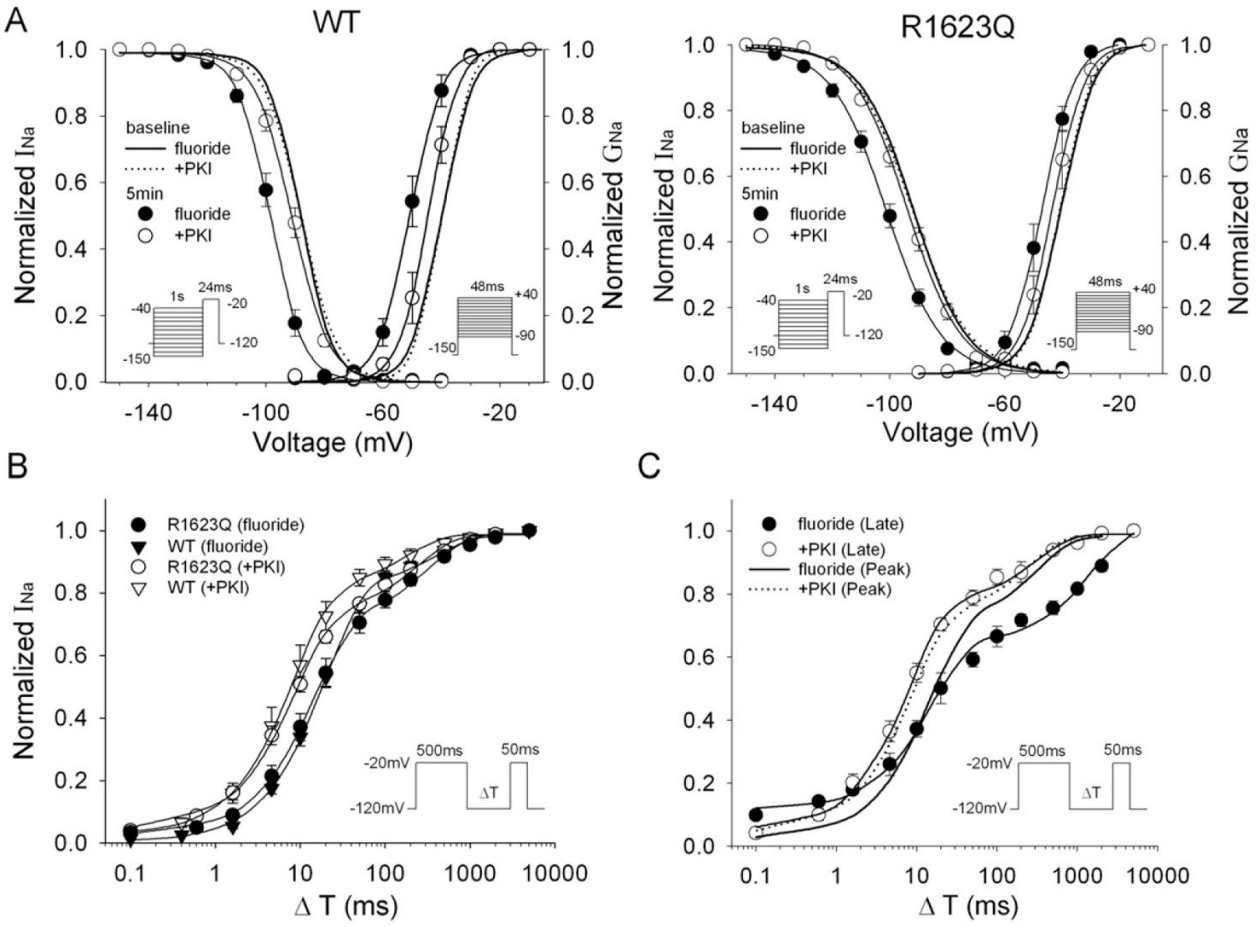

Fig. 4.

Kinetic modulation by fluoride. (A) Steady-state inactivation and activation relationships for WT and R1623Q channels. Pulse protocols for inactivation and for activation are indicated in *insets*. Lines represent fits to a Boltzmann function. (B and C) Time course of recovery from inactivation for peak I_{Na} in WT and R1623Q channels (B) and for late I_{Na} in R1623Q channels (C). Recovery of peak I_{Na} in R1623Q channels is duplicated in (C) for comparison. The pulse protocol for the recovery from inactivation is indicated in *insets*. Peak I_{Na} and late I_{Na} measured at 50 ms were normalized to the maximum current recorded in the absence of a conditioning pulse and plotted against the recovery time (ΔT) on a logarithmic axis. Lines represent the fitting with double-exponential function. Data are mean±SEM. Values of parameters are summarized in Tables 2 and 3.

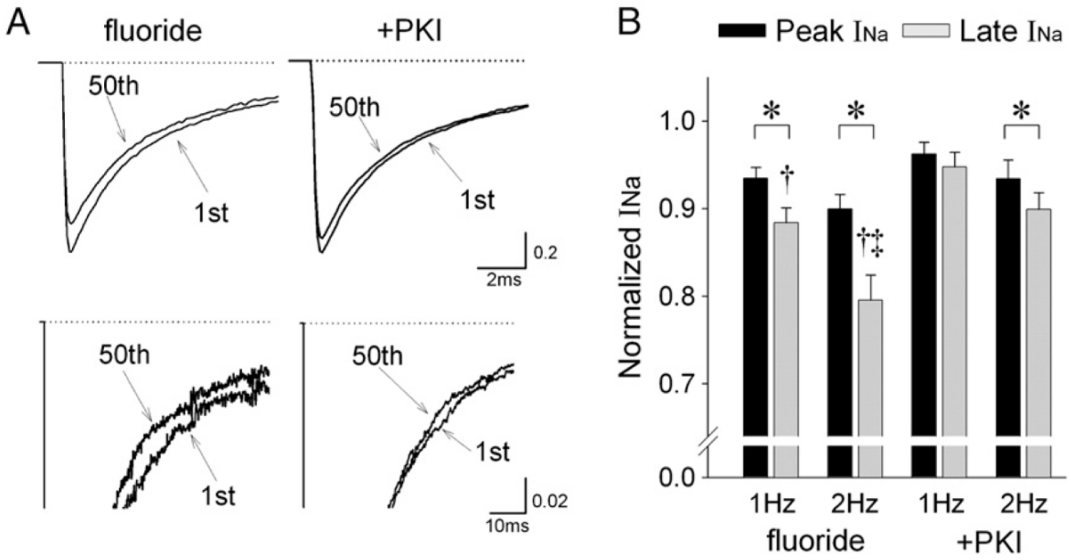

Fig. 5.

Effects of fluoride on the frequency-dependence of peak and late I_{Na} in R1623Q channels. (A) Representative current recordings in response to trains of 50 pulses with fluoride in the presence or absence of PKI (20 μM) at 2 Hz. Currents were elicited by 50 ms step pulses to −20 mV from a holding potential of −120 mV. Upper panels: superimposed current traces from the 1st and 50th pulses in the train to demonstrate peak I_{Na}. Lower panels: the same traces at different amplitude (peak I_{Na} off scale) and time resolution to demonstrate late I_{Na}. (B) Summary data showing frequency-dependent reduction of peak and late I_{Na} at 1 Hz and 2 Hz. The current amplitudes for peak and late I_{Na} in response to the last five pulses of the train were averaged and normalized to the first pulse in the train. Data are mean±SEM. fluoride: 1 Hz (n=11), 2 Hz (n=10), +PKI: 1 Hz (n=10), 2 Hz (n=10). *P<0.05 between peak and late I_{Na}, †P<0.05 compared with +PKI, ‡P<0.05 compared with 1 Hz.

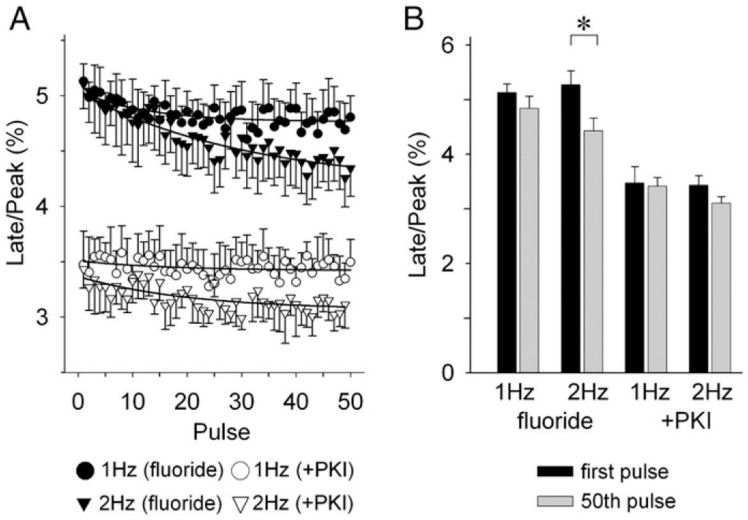

Fig. 6.

Overall effects of fluoride on late I_{Na}. (A) Time course of frequency-dependent reduction of the relative amplitude of late I_{Na} (peak/late I_{Na}) by fluoride in the presence (open symbols) or absence (closed symbols) of PKI (20 μM). (B) Summary data for the relative amplitude of late I_{Na} at first pulse and 50th pulse in a train. Data are mean± SEM. fluoride: 1 Hz (n=11), 2 Hz (n=10), +PKI: 1 Hz (n=10), 2 Hz (n=10). *P<0.05.

Table 1

Parameters for macroscopic current decay

	WT (pCPT-cAMP+fluoride)		R1623Q (pCPT-cAMP+fluoride)		R1623Q (fluoride)		R1623Q (fluoride+PKI)	
	Baseline	**10 min**	**Baseline**	**10 min**	**Baseline**	**10 min**	**Baseline**	**10 min**
τ_f (ms)	0.51±0.04	0.51±0.02	3.3±0.2	3.6±0.2	3.4±0.3	3.9±0.2	3.6±0.2	3.5±0.2
τ_s (ms)	3.2±0.4	3.5±0.5	14.9±0.4	18.1±0.9*	15.9±1.0	19.1±1.1*	15.2±1.0	16.0±0.9
A_s	0.13±0.03	0.12±0.02	0.28±0.02	0.32±0.02	0.36±0.03	0.37±0.02	0.35±0.02	0.37±0.03
Offset (×100)			0.8±0.1	1.1±0.1*	0.9±0.2	1.4±0.1*	0.8±0.4	0.8±0.5
n	5		5		5		6	

Data are mean±SEM. *n*, number of experiments; τ_f, fast time constant; τ_S, slow time constant; A_S, fractional amplitude of slow component.

*P<0.05 compared with at baseline.

Table 2

Slope factors and $V_{1/2}$ of activation and inactivation

	WT (fluoride)		WT (fluoride+PKI)		R1623Q (fluoride)		R1623Q (fluoride+PKI)	
	Baseline	**10 min**	**Baseline**	**10 min**	**Baseline**	**10 min**	**Baseline**	**10 min**
	Activation				Activation			
Slope factor	4.9±0.2	4.9±0.3	4.4±0.3	4.5±0.4	5.3±0.2	5.2±0.2	4.7±0.4	4.8±0.4
$V_{1/2}$ (mV)	−39.6±1.2	−50.4±1.7*	−39.8±1.1	−44.3±1.4*	−40.5±1.2	−47.7±1.7*	−40.5±1.8	−43.2±2.0
Shift in $V_{1/2}$	−10.8±1.1		−4.5±1.3†		−7.2±1.0		−2.7±0.4†	
n	8		6		5		7	
	Inactivation				Inactivation			
Slope factor	−5.1±0.3	−5.3±0.1	−5.9±0.4	−5.9±0.3	−9.1±0.5	−9.1±0.4	−9.6±0.3	−9.3±0.2
$V_{1/2}$ (mV)	−88.0±0.9	−98.3±1.2*	−88.0±0.6	−91.7±0.6*	−91.8±0.8	−98.0±0.8*	−91.3±1.1	−93.8±1.2
Shift in $V_{1/2}$	−10.3±0.8		−3.6±0.5†		−6.2±0.6		−2.5±0.5†	
n	8		7		7		7	

Data are mean±SEM. *n*, number of experiments; $V_{1/2}$, half-maximum voltage.

*$P<0.05$ compared with at baseline.

†$P<0.05$ compared with fluoride.

Table 3

Parameters for recovery from inactivation

	WT		R1623Q-peak		R1623Q-late	
	Fluoride	**Fluoride+PKI**	**Fluoride**	**Fluoride+PKI**	**Fluoride**	**Fluoride+PKI**
τ_f (ms)	18.3±1.9*	9.3±1.9	16.4±3.6*	8.8±1.1	17.5±3.3*	7.8±1.1
τ_s (ms)	377±71	237±62	360±32	252±28	1663±195*	290±83
A_s	0.17±0.01	0.18±0.02	0.27±0.03	0.26±0.02	0.37±0.02*	0.26±0.03
Offset					0.11±0.01*	0.04±0.01
n	8	5	6	7	6	8

Data are mean±SEM. *n*, number of experiments; τ_f, fast time constant; τ_S, slow time constant; A_S, fractional amplitude of slow component.

*P<0.05 compared with +PKI.

Life Sci. Author manuscript; available in PMC 2009 September 21.